Modification of Dzyaloshinskii-Moriya-Interaction-Stabilized Domain Wall Chirality by Driving Currents

G. V. Karnad,[1] F. Freimuth,[2] E. Martinez,[3] R. Lo Conte,[1,4] G. Gubbiotti,[5] T. Schulz,[1] S. Senz,[6] B. Ocker,[7] Y. Mokrousov,[1,2,4,*] and M. Kläui[1,4,†]

[1]*Institut für Physik, Johannes Gutenberg-Universität, Staudinger Weg 7, 55128 Mainz, Germany*
[2]*Peter Grünberg Institut and Institute for Advanced Simulation, Forschungszentrum Jülich and JARA, 52425 Jülich, Germany*
[3]*Departamento Fisica Aplicada, Facultad de Ciencias, University of Salamanca, 37008 Salamanca, Spain*
[4]*Graduate School of Excellence "Materials Science in Mainz" (MAINZ), Staudinger Weg 9, 55128 Mainz, Germany*
[5]*Istituto Officina dei Materiali del CNR (CNR-IOM), Sede Secondaria di Perugia, c/o Dipartimento di Fisica e Geologia, Universitá di Perugia, I-06123 Perugia, Italy*
[6]*Max-Planck-Institut für Mikrostrukturphysik, 06120 Halle(Saale), Germany*
[7]*Singulus Technology AG, 63796 Kahl am Main, Germany*

(Received 6 June 2018; published 3 October 2018)

We measure and analyze the chirality of Dzyaloshinskii-Moriya-interaction (DMI) stabilized spin textures in multilayers of $Ta|Co_{20}F_{60}B_{20}|MgO$. The effective DMI is measured experimentally using domain wall motion measurements, both in the presence (using spin-orbit torques) and absence of driving currents (using magnetic fields). We observe that the current-induced domain wall motion yields a change in effective DMI magnitude and opposite domain wall chirality when compared to field-induced domain wall motion (without current). We explore this effect, which we refer to as current-induced DMI, by providing possible explanations for its emergence, and explore the possibility of its manifestation in the framework of recent theoretical predictions of DMI modifications due to spin currents.

DOI: 10.1103/PhysRevLett.121.147203

The Dzyaloshinskii-Moriya-interaction (DMI) [1–4] is an asymmetric exchange interaction found in systems possessing inversion asymmetry in bulk as well as in multilayers (interfacial origin). The magnitude of the interfacial DMI can be influenced by changing materials [5,6], layer ordering [7], ferromagnetic layer thickness [8], and by interface modification [7]. Experimentally, there are several methods by which DMI has been measured [5,9–17].

Recently, a very intuitive relationship between the DMI and the ground-state spin current has been found [18,19]. The ground-state spin current represents the spin current present in an equilibrium system, in the absence of a net electric field. It was shown that a linear contribution of the spin-orbit interaction to the ground-state spin current is dominated by the Zeeman interaction of the spin-orbit field with the misalignment of the spins, which the conduction electrons acquire as they propagate in the spin textures [19], resulting in an observation that to first order in spin orbit the DMI is given by the ground-state spin currents. This finding directly suggests the possibility to tailor DMI by exciting the nonequilibrium spin currents in the system, e.g., by applying an external electric field $\boldsymbol{E}$. It was shown that the corresponding effect of the DMI modified by spin current could be realized in a system where the spin polarization ($\boldsymbol{\sigma}$) of the spin current is perpendicular to the magnetization ($\boldsymbol{m}$), which makes magnetic multilayers with perpendicular magnetic anisotropy the ideal candidates for the experimental observation of this new phenomenon [19]. However, as was roughly estimated for Co/Pt bilayers [19], even for large spin currents of the order of 10^7 A/cm^2 $\hbar/e$, the resulting change of the DMI is on the order of 0.05 meV per atom, which is smaller than the DMI of the system in equilibrium by 2 orders of magnitude. This implies that to observe this effect large spin-current densities and/or small values of the DMI in equilibrium are required.

With this work we aim at exploring the effect that an electrical current can have on the DMI. Recent studies [8,20,21] have reported differences in magnitude and/or sign when comparing DMI parameter extracted by techniques with and without the use of current. To study this, we perform domain wall (DW) motion measurements, magnetic field driven and current driven, and probe the influence of the driving current on the effective measured DMI-induced DW chirality. DW motion based techniques provide the possibility to perform experiments by driving the DWs either with magnetic field or with currents, allowing for a direct comparison when using the same spin structures. We choose a well-characterized system of $Ta(5)|Co_{20}F_{60}B_{20}(0.8)|MgO(2)$ (all thicknesses in nm), which has a large perpendicular anisotropy [22], relatively small DMI [6,9,13,23], and a sizable spin Hall current source (Ta) [24].

Experiments proposed to quantify the DMI using field-induced domain wall motion (FIDWM) simultaneously apply both an out-of-plane (B_z, to drive the DW motion) and an in-plane (B_x to asymmetrically modify the DW energy density, σ) magnetic field [7,10,25]. The sign of the in-plane field exploits the chirality induced in the DWs by the DMI and thus selectively increases or decreases the DW energy, which directly affects the field ($\mu_0 H_z$) driven wall velocity. This technique was motivated [7] by the opportunity to eliminate the spin-orbit torques (SOTs) in the measurement [6,13] of DMI. However, it was shown [26,27] that this technique is not universally applicable and is dependent on the specifics of the material system, interfaces, and motion regime, and which could be overcome by measuring systems in the flow regime, where pinning would not dominate the DW dynamics. This anomalous behavior can also be eliminated by using a system with low pinning [28]. Jué *et al.* observed that in a system such as Pt|Co|Pt where the symmetry is weakly broken and has negligible DMI, experimental signals could only be explained by a chiral damping term [27].

Here, we perform asymmetric bubble expansion measurement (Fig. 1) and observe that the application of an in-plane field indeed breaks the symmetry of the DW energy.

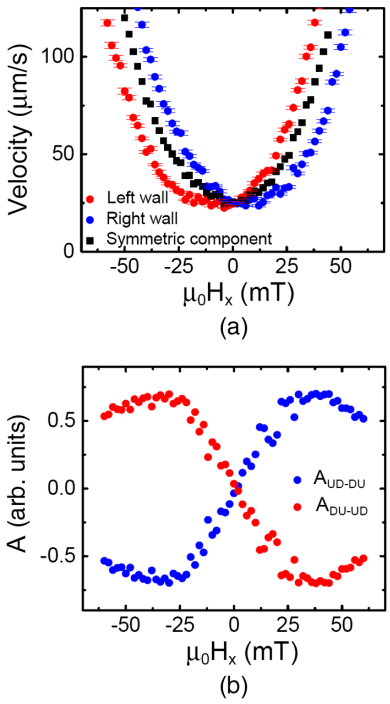

FIG. 1. Field-induced domain wall motion experiment. (a) DW velocity as a function of in-plane magnetic field ($\mu_0 H_x$), where the DW is driven by an out-of-plane magnetic field ($\mu_0 H_z$) of 1.5 mT. The symmetric component (black squares) is given by, $S = (v_{UD} + v_{DU})/2$, where the subscript UD refers to up-down DW and DU refers to down-up DW. (b) The antisymmetric (blue dots, A_{UD-DU}; red dots, A_{DU-UD}) component of the DW velocity, where the antisymmetric component is given by $A_{UD-DU} = 2(v_{UD} - v_{DU})/(v_{UD} + v_{DU})$ (in arb. units, a.u.).

We observe an asymmetric expansion of a bubble-shaped domain [29]. This indicates the presence of a chiral contribution dictating the DW dynamics: chiral energy (DMI) or chiral dissipation (chiral damping). We explore these possibilities and separate the chiral effects [27] by decomposing the DW velocities measured with respect to $\mu_0 H_x$ into (a) a symmetric component $S = (v_{UD} + v_{DU})/2$ and (b) an antisymmetric component $A_{UD-DU} = 2(v_{UD} - v_{DU})/(v_{UD} + v_{DU})$, as plotted in Fig. 1. The antisymmetric component clearly confirms the presence of a chiral term (either in energy or dissipation) in the system. We perform analytical calculations [29] to check the behavior of the DW velocities in the presence of only a chiral energy (DMI) in the system and observe that the numerical calculations reproduce the experimental observations. If the antisymmetry (A) in the system was a result of the chiral damping, this would result in DW velocity curves which would not be possible to overlap despite translation along the x axis [27]. However, we observe that the DW velocities are symmetric around $|\mu_0 H_{\mathrm{DMI}}|$ and overlap by translating along the x axis. This indicates that the dominant chiral effect in the system is the DMI, which is at the origin of the chiral energy in the system. The extracted $\mu_0 H_{\mathrm{DMI}} = 8.8 \pm 2\,\mathrm{mT}$, is the average of the in-plane field at which the DW velocity of the left and right DWs are the lowest (Bloch DW configuration) [7,10]. The effective DMI can be calculated by $D_{\mathrm{eff}} = \mu_0 H_{\mathrm{DMI}} M_s \Delta$, where saturation magnetization $M_s = 0.705 \times 10^6$ A/m, and the DW width $\Delta = 5.35$ nm. This allows us to extract an effective DMI in the system, $D_{\mathrm{eff,field}} = +33 \pm 7.5\ \mu\mathrm{J/m^2}$. The symmetry of the asymmetric expansion also indicates that the system is right-handed.

To evaluate the influence of current on DWs and hence on the DMI, we perform current-induced domain wall motion (CIDWM) under the application of in-plane magnetic fields (details in the Supplemental Material [29]). This method [6,13] allows us to observe the influence of the SOTs on the DW texture. The direction of the CIDWM is governed by two important parameters: spin Hall angle (intrinsic property [41] of the heavy metal) and the chirality of the Néel wall induced by the DMI [11,12,42]. We find from SOT measurements [43] that the sign of the spin Hall angle of Ta is negative, which is in agreement with previous reports [24,41]. Furthermore, from the FIDWM reported above, we know that the DMI is of relatively small magnitude (see also Brillouin light scattering measurements [29]) and is right-handed (see previous, $D = +33\ \mu\mathrm{J/m^2}$) in our system. Based on this, we expect the DWs to move in the direction of charge current.

We perform the CIDWM experiments on an array of nanowires (NWs) patterned on a thin film sample [29]. The minimum current density to perform the experiment is dictated by the depinning current and the maximum current is limited by the thermal nucleation events. We observe that the DWs move along the direction of electron flow, which

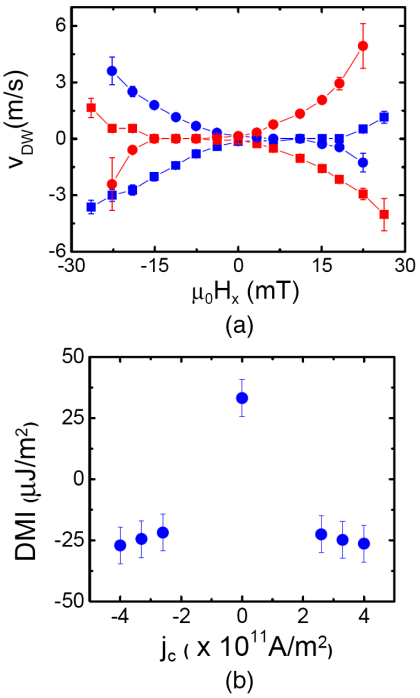

FIG. 2. Current-induced domain wall motion experiment. (a) DW velocities (up-down, blue; down-up, red) are measured under the application of an in-plane magnetic field. It is measured for a current density of $+3.3 \times 10^{11}$ A/m^2 (squares) and -3.3×10^{11} A/m^2 (dots). (b) The effective DMI for different current densities. A switching of DMI chirality is observed under injection of driving current.

is opposite to the predicted direction. We observe that the velocity also increases on increasing the current density. Additionally, we note that the velocities for FIDWM and CIDWM are consistent as the dampinglike effective fields $\mu_0 H_{\mathrm{DL}}$ that correspond to the current densities used are much larger than the magnetic field used for FIDWM. To check for the presence and quantify the DMI, we perform the measurements for a range of current densities, which provides stable DW motion without nucleation events (also in the presence of $\mu_0 H_x$). We observe that the DW motion is indeed sensitive to the direction of the in-plane field [see Fig. 2(a)]. The DWs stop moving for a certain in-plane field and then switch the direction of motion when the applied $\mu_0 H_x$ is high. This stopping magnetic field can be interpreted as the effective DMI field, where the wall has a Bloch character and thus does not move as the effective SOT is zero, allowing us to extract an effective DMI field and a resultant DMI parameter, D [6]. This confirms that there is indeed DMI present in the system, and the motion of the DWs in the system is due to SOTs. The DW motion direction, however, can only be explained by an opposite chirality [see Eqs. (S2) and (S3) in Supplemental Material [29]] compared to FIDWM. This indicates that the DMI in the system under the influence of current is switched to a left-handed system and reaches a value of $D_{\mathrm{eff,current}} = -26 \pm 7.5\ \mu\mathrm{J/m}^2$ at 4×10^{11} A/m^2.

The results of the effective DMI as a function of current density [see Fig. 2(b)] show a nonlinear dependence, and we find in the experiment that the current-induced change of DMI is manifestly independent of the polarity of the current [see Fig. 2(b)]. This is expected, because symmetry rules out a current-induced modification of DMI linear in the applied electric field in the magnetic bilayer geometry considered here. To illustrate this we show in Fig. 3(a) a chiral down-up Néel-type DW in the presence of an electric field $\boldsymbol{E}$ pointing to the right and a chiral up-down DW in the presence of an electric field $\boldsymbol{E}$ pointing to the left. Since a rotation around the interface normal by 180° maps the two situations onto each other, the DW width (for details, see discussion later) is not affected to first order in $\boldsymbol{E}$. Consequently, there cannot be a current-induced change of DMI linear in $\boldsymbol{E}$ in this bilayer geometry.

The anomaly of sign difference [20,21] and difference in magnitude [8] in DMI has been mentioned in literature before. Fundamentally, the variation of the sign of DMI can be expected to arise from various origins. In addition to the current-induced modifications to the DMI brought by various spin currents which an electric field can induce in this complex interfacial system, it is also expected that there is heating in the wires (increase of ≈50 K for the

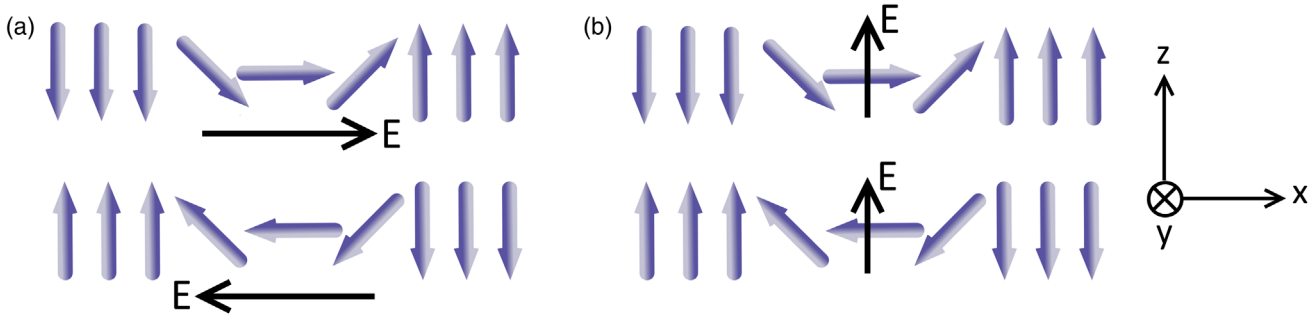

FIG. 3. (a) A left-handed Néel-type down-up DW in the presence of an electric field pointing to the right is symmetry equivalent to a left-handed Néel-type up-down DW in the presence of an electric field pointing to the left. (b) A left-handed Néel-type down-up DW in the presence of an electric field in z direction is symmetry equivalent to a left-handed Néel-type up-down DW in the presence of an electric field in z direction.

maximum current density applied here) caused by the current. This can increase the temperature [6] and can change the DMI [44]. The increase in a temperature with current density would result in reduction of ground-state DMI [44], and thus the importance of the DMI contribution from current injection would increase with increasing current density and thus heating. This is qualitatively in line with our observations that the amplitude of the observed DMI increases with increasing current density.

Other possible reasons for the DMI change include the change in sign of the dampinglike torque, effects of the fieldlike torque on DW motion which were not taken into account, Oersted field, chiral damping, and, importantly the effects of the spin-transfer torque (STT) on the DW motion. We briefly discuss some of these possibilities.

Chiral damping.—Chiral damping and DMI have been proposed to share the same origin. The dominance of the chiral dissipation has been observed in a structure with minimal symmetry breaking [27]. However, the system of $Ta|Co_{20}F_{60}B_{20}|MgO$ has a large structural asymmetry and therefore the magnitude of the chiral damping can be expected to be minimal. Despite the issue of the FIDWM being in the creep regime, it should be noted that the reported sign of the DMI itself is consistent [26,45] in the creep and flow regimes.

Oersted field.—Oersted field can be expected to influence the DW motion. This is especially true if the symmetry of field created along the NWs would be along the z axis. However, while we calculate that the Oersted field is negligible, we eliminate its influence by measuring in an array of NWs—the neighboring NWs will largely compensate for any Oersted field in the structure. The influence of Oersted fields from the injection pads is also avoided by measuring at the central area of the NWs where the Oersted field, if any, would be zero. It should be noted that we do not observe any substantial difference in DW velocities in any of the NWs or along their individual length.

Spin-transfer torque.—During the injection of current pulses, due to the metallic nature of the stack there is always current shunting through the ferromagnetic layer as well. Because of the direction of CIDWM being with the electron flow direction, it would assist the effect of the SOT. While the effect of the dampinglike torque is sensitive to the DW structure, the bulk STT is not. Irrespective of the chirality or structure of the DW, the motion would always be in the direction of the electron flow. However, we observe that the DW motion measured in our stacks is highly sensitive to the chirality of the DW and stops moving when the wall is tuned to the Bloch state. Additionally, the current density in the FM is expected to be small, and the irrelevance of STT for CIDWM in such thin multilayer stacks was also previously reported [11]. In addition, due to the large thickness of Ta (5 nm), we estimate the spin-current density through CoFeB to be negligible ($\ll$14% of the total current density), suggesting a negligible STT. However, in the extreme case of an enhanced STT, the direction of wall motion can flip sign, since the in-plane field changes the DW width and thus the nonadiabatic spin-transfer torque also can potentially change sign [46] and move the wall in the opposite direction than the bulk STT. However, it should be noted that the scenario presented by Je *et al.* [46] has a spin Hall effect (SHE) compensated structure resulting in STT being the main driving force, unlike our case of a large SHE.

Finally, we propose examples for geometries in which symmetry allows for a current-induced modification of DMI linear in $\boldsymbol{E}$ according to the model put forward by Freimuth *et al.* [19]. Potentially, this could lead to a more pronounced effect as compared to the effect that we observe in this work. As a first example, we illustrate in Fig. 3(b) the case in which the electric field is perpendicular to the wall. Since rotation by 180° around the interface normal does not affect the electric field vector in this case, a current-induced modification of DMI that is linear in $\boldsymbol{E}$ is allowed in this case.

In order to obtain a systematic tool for the prediction of current-induced DMI, we introduce the DMI coefficients D_{ij} such that

$$\delta F(\boldsymbol{r}) = \sum_{ij} D_{ij}\hat{\boldsymbol{e}}_i \cdot \left(\hat{\boldsymbol{M}} \times \frac{\partial \hat{\boldsymbol{M}}}{\partial r_j}\right) \tag{1}$$

is the change of energy density due to DMI, where $\hat{\boldsymbol{M}}(\boldsymbol{r})$ is the magnetization direction at position $\boldsymbol{r}$ and $\hat{\boldsymbol{e}}_i$ is a unit vector pointing in the ith Cartesian direction. The DMI coefficients D_{ij} have the symmetry properties of an axial tensor of second rank [47,48]. Similarly, spin currents are described by axial tensors of second rank. Therefore, when symmetry allows for a spin current J^i_j, where j labels the direction of current flow and i the orientation of the spins in the spin current, symmetry implies that the DMI coefficient D_{ij} can be nonzero as well. If the electric field $\boldsymbol{E}$ induces a spin current J^i_j in a magnetic system, we may therefore expect that the DMI coefficient D_{ij} changes as well. This provides a systematic tool for predicting cases in which DMI changes proportional to $\boldsymbol{E}$ can be observed. This analogy between the spin current J^i_j and the DMI coefficient D_{ij} follows from symmetry considerations alone, because both quantities are axial tensors of second rank, and is therefore generally valid. However, it has been shown recently that at first order perturbation theory in the spin-orbit interaction without applied electric field even $J^i_j = -D_{ij}$ holds [18,19]; i.e., the DMI coefficient is determined by the ground-state spin current. We can therefore understand why $\boldsymbol{E}$ can induce a change of DMI in Fig. 3(b) from our knowledge of the SHE: For the Néel-type wall in Fig. 3(b), the wall width depends on D_{yx}, and an electric field in the z direction is expected to induce a spin current J^y_x via the SHE. This mechanism for the current-induced DMI could be

particularly relevant in the multilayer geometry, in which the magnetic layers are coupled by an antisymmetric Ruderman-Kittel-Kasuya-Yosida-type of DMI [49].

Without applied electric field, D_{ij} is even under time reversal [47]. Similarly, ground-state spin currents are time-reversal-even. The spin current generated by the SHE is time-reversal-even as well. In magnetic systems, applied electric fields may also induce spin currents that are time-reversal-odd. An example is the generation of a spin current by a polarizing magnet in a spin-valve setup, in which case the spin current changes sign when the magnetization of the polarizing magnet is reversed. Such time-reversal-odd spin currents may induce changes of DMI as well. Therefore, despite the absence of a complete overarching theory to understand our results, the experimental results indicate that the DMI can indeed be influenced by the injection of currents.

We acknowledge support by the EU (Marie Curie ITN WALL -FP7-PEOPLE-2013-ITN 608031), the DFG (SFB TRR 173), and Graduate School of Excellence Materials Science in Mainz (MAINZ) GSC 266. G. V. K. would like to acknowledge the funding received by the EU (Erasmus Mundus Master Nanoscience and Nanotechnology-2010-0119 R 05-28/001, Marie Curie ITN WALL -FP7-PEOPLE-2013-ITN 608031). The work by E. M. was additionally supported by Projects No. MAT2014-52477-C5-4-P and No. MAT2017-87072-C4-1-P from the Spanish government, and Project No. SA090U16 from the Junta de Castilla y Leon. Y. M. and F. F. gratefully acknowledge computing time on the supercomputers of Jülich Supercomputing Center and RWTH Aachen University as well as funding by Deutsche Forschungsgemeinschaft (MO 1731/5-1).

*y.mokrousov@fz-juelich.de
†klaeui@uni-mainz.de

[1] I. Dzyaloshinsky, J. Phys. Chem. Solids **4**, 241 (1958).
[2] T. Moriya, Phys. Rev. **120**, 91 (1960).
[3] A. Fert, Mater. Sci. Forum **59–60**, 439 (1990).
[4] A. Soumyanarayanan, N. Reyren, A. Fert, and C. Panagopoulos, Nature (London) **539**, 509 (2016).
[5] G. Chen, T. Ma, A. N'Diaye, H. Kwon, C. Won, Y. Wu, and A. Schmid, Nat. Commun. **4**, 2671 (2013).
[6] J. Torrejon, J. Kim, J. Sinha, S. Mitani, M. Hayashi, M. Yamanouchi, and H. Ohno, Nat. Commun. **5**, 4655 (2014).
[7] A. Hrabec, N. A. Porter, A. Wells, M. J. Benitez, G. Burnell, S. McVitie, D. McGrouther, T. A. Moore, and C. H. Marrows, Phys. Rev. B **90**, 020402 (2014).
[8] R. L. Conte, G. V. Karnad, E. Martinez, K. Lee, N.-H. Kim, D.-S. Han, J.-S. Kim, S. Prenzel, T. Schulz, C.-Y. You *et al.*, AIP Adv. **7**, 065317 (2017).
[9] J.-P. Tetienne, T. Hingant, L. J. Martnez, S. Rohart, A. Thiaville, L. H. Diez, K. Garcia, J.-P. Adam, J.-V. Kim, J.-F. Roch *et al.*, Nat. Commun. **6**, 6733 (2015).
[10] S.-G. Je, D.-H. Kim, S.-C. Yoo, B.-C. Min, K.-J. Lee, and S.-B. Choe, Phys. Rev. B **88**, 214401 (2013).
[11] S. Emori, U. Bauer, S. Ahn, E. Martinez, and G. Beach, Nat. Mater. **12**, 611 (2013).
[12] K.-S. Ryu, L. Thomas, S.-H. Yang, and S. Parkin, Nat. Nanotechnol. **8**, 527 (2013).
[13] S. Rohart and A. Thiaville, Phys. Rev. B **88**, 184422 (2013).
[14] J. Cho, N.-H. Kim, S. Lee, J.-S. Kim, R. Lavrijsen, A. Solignac, Y. Yin, D.-S. Han, N. J. J. van Hoof, H. J. M. Swagten *et al.*, Nat. Commun. **6**, 7635 (2015).
[15] M. Belmeguenai, J.-P. Adam, Y. Roussigné, S. Eimer, T. Devolder, J.-V. Kim, S. M. Cherif, A. Stashkevich, and A. Thiaville, Phys. Rev. B **91**, 180405 (2015).
[16] J. M. Lee, C. Jang, B.-C. Min, S.-W. Lee, K.-J. Lee, and J. Chang, Nano Lett. **16**, 62 (2016).
[17] S. Tacchi, R. E. Troncoso, M. Ahlberg, G. Gubbiotti, M. Madami, J. Åkerman, and P. Landeros, Phys. Rev. Lett. **118**, 147201 (2017).
[18] T. Kikuchi, T. Koretsune, R. Arita, and G. Tatara, Phys. Rev. Lett. **116**, 247201 (2016).
[19] F. Freimuth, S. Blügel, and Y. Mokrousov, Phys. Rev. B **96**, 054403 (2017).
[20] S. Chenattukuzhiyil, Ph.D. thesis, Universite Grenoble Alpes, 2015.
[21] R. Soucaille, M. Belmeguenai, J. Torrejon, J.-V. Kim, T. Devolder, Y. Roussigné, S.-M. Chérif, A. A. Stashkevich, M. Hayashi, and J.-P. Adam, Phys. Rev. B **94**, 104431 (2016).
[22] S. Ikeda, K. Miura, H. Yamamoto, K. Mizunuma, H. Gan, M. Endo, S. Kanai, J. Hayakawa, F. Matsukura, and H. Ohno, Nat. Mater. **9**, 721 (2010).
[23] G. V. Karnad, E. Martinez, M. Voto, T. Schulz, B. Ocker, D. Ravelosona, and M. Kläui, arXiv:1806.00294.
[24] L. Liu, C.-F. Pai, Y. Li, H. Tseng, D. Ralph, and R. Buhrman, Science **336**, 555 (2012).
[25] D.-H. Kim, S.-C. Yoo, D.-Y. Kim, B.-C. Min, and S.-B. Choe, Sci. Rep. **7**, 45498 (2017).
[26] M. Vaňatka, J.-C. Rojas-Sánchez, J. Vogel, M. Bonfim, M. Belmeguenai, Y. Roussigné, A. Stashkevich, A. Thiaville, and S. Pizzini, J. Phys. Condens. Matter **27**, 326002 (2015).
[27] E. Jué, C. Safeer, M. Drouard, A. Lopez, P. Balint, L. Buda-Prejbeanu, O. Boulle, S. Auffret, A. Schuhl, A. Manchon *et al.*, Nat. Mater. **15**, 272 (2016).
[28] C. Burrowes, N. Vernier, J.-P. Adam, L. H. Diez, K. Garcia, I. Barisic, G. Agnus, S. Eimer, J.-V. Kim, T. Devolder *et al.*, Appl. Phys. Lett. **103**, 182401 (2013).
[29] See Supplemental Material at http://link.aps.org/supplemental/10.1103/PhysRevLett.121.147203, which includes Refs. [6,10,15,17,30–40], for details on sample preparation, experimental methods, and additional experimental data.
[30] S. Tarasenko, A. Stankiewicz, V. Tarasenko, and J. Ferr, J. Magn. Magn. Mater. **189**, 19 (1998).
[31] V. P. Amin and M. D. Stiles, Phys. Rev. B **94**, 104420 (2016).
[32] M. Madami, G. Gubbiotti, S. Tacchi, and G. Carlotti, *Solid State Physics* (Academic Press, New York, 2012), Vol. 63, pp. 79–150.
[33] A. K. Chaurasiya, S. Choudhury, J. Sinha, and A. Barman, Phys. Rev. Applied **9**, 014008 (2018).

[34] J. R. Dutcher, J. F. Cochran, I. Jacob, and W. F. Egelhoff, Phys. Rev. B **39**, 10430 (1989).
[35] G. Gubbiotti, G. Carlotti, M. G. Pini, P. Politi, A. Rettori, P. Vavassori, M. Ciria, and R. C. O'Handley, Phys. Rev. B **65**, 214420 (2002).
[36] G. Gubbiotti, G. Carlotti, S. Tacchi, M. Madami, T. Ono, T. Koyama, D. Chiba, F. Casoli, and M. G. Pini, Phys. Rev. B **86**, 014401 (2012).
[37] M. Munakata, S.-I. Aoqui, and M. Yagi, IEEE Trans. Magn. **41**, 3262 (2005).
[38] V. Sokalski, M. T. Moneck, E. Yang, and J.-G. Zhu, Appl. Phys. Lett. **101**, 072411 (2012).
[39] R. A. Khan, P. M. Shepley, A. Hrabec, A. W. J. Wells, B. Ocker, C. H. Marrows, and T. A. Moore, Appl. Phys. Lett. **109**, 132404 (2016).
[40] M. Cecot, Ł. Karwacki, W. Skowroński, J. Kanak, J. Wrona, A. Żywczak, L. Yao, S. van Dijken, J. Barnaś, and T. Stobiecki, Sci. Rep. **7**, 968 (2017).
[41] T. Tanaka, H. Kontani, M. Naito, T. Naito, D. S. Hirashima, K. Yamada, and J. Inoue, Phys. Rev. B **77**, 165117 (2008).
[42] A. V. Khvalkovskiy, V. Cros, D. Apalkov, V. Nikitin, M. Krounbi, K. A. Zvezdin, A. Anane, J. Grollier, and A. Fert, Phys. Rev. B **87**, 020402 (2013).
[43] T. Schulz, K. Lee, B. Krüger, R. Lo Conte, G. V. Karnad, K. Garcia, L. Vila, B. Ocker, D. Ravelosona, and M. Kläui, Phys. Rev. B **95**, 224409 (2017).
[44] S. Kim, K. Ueda, G. Go, P.-H. Jang, K.-J. Lee, A. Belabbes, A. Manchon, M. Suzuki, Y. Kotani, T. Nakamura *et al.*, Nat. Commun. **9**, 1648 (2018).
[45] D.-H. Kim, S.-C. Yoo, D.-Y. Kim, B.-C. Min, and S.-B. Choe, arXiv:1608.01762.
[46] S.-G. Je, S.-C. Yoo, J.-S. Kim, Y.-K. Park, M.-H. Park, J. Moon, B.-C. Min, and S.-B. Choe, Phys. Rev. Lett. **118**, 167205 (2017).
[47] F. Freimuth, S. Blügel, and Y. Mokrousov, J. Phys. Condens. Matter **26**, 104202 (2014).
[48] F. Freimuth, S. Blügel, and Y. Mokrousov, J. Phys. Condens. Matter **28**, 316001 (2016).
[49] M. Belmeguenai, H. Bouloussa, Y. Roussigné, M. S. Gabor, T. Petrisor, C. Tiusan, H. Yang, A. Stashkevich, and S. M. Chérif, Phys. Rev. B **96**, 144402 (2017).